Powers, J. C., Gupton, B. F., Harley, A. D., Nishino, N., & Whitley, R. F. (1977) *Biochim. Biophys. Acta 485*, 156-166.
Reilly, C. F., Tewksbury, D. A., Schechter, N. M., & Travis, J. (1982) *J. Biol. Chem. 257*, 8619-8622.
Schechter, I., & Berger, A. C. (1967) *Biochem. Biophys. Res. Commun. 27*, 157-162.
Schechter, N. M., Fraki, J. E., Geesin, J. C., & Lazarus, G. S. (1983) *J. Biol. Chem. 258*, 2973-2978.
Stein, R. L., Viscarello, B. R., & Wildonger, R. A. (1984) *J. Am. Chem. Soc. 106*, 796-798.
Szabo, G. C., Pozsgay, M., Gaspar, R., & Elodi, P. (1980) *Acta Biochim. Biophys. Acad. Sci. Hung. 15*, 263-273.
Tanaka, T., Minematsu, Y., Reilly, C. F., Travis, J., & Powers, J. C. (1985) *Biochemistry* (preceding paper in this issue).
Travis, J., Bowen, J., & Baugh, R. (1978) *Biochemistry 17*, 5651-5656.
Umezawa, H., & Aoyagi, T. (1977) in *Proteases in Mammalian Cells and Tissues* (Barrett, A. J., Ed.) pp 637-662, North-Holland Publishing Co., New York.
Wintroub, B. U., Klickstein, L. B., Dzau, V. J., & Watt, K. W. K. (1984) *Biochemistry 23*, 227-232.
Woodbury, R. G., & Neurath, H. (1978) *Biochemistry 17*, 4298-4304.
Woodbury, R. G., & Neurath, H. (1980) *FEBS Lett. 114*, 189-196.
Woodbury, R. G., Katunuma, N., Kobayashi, K., Tatani, K., & Neurath, H. (1978a) *Biochemistry 17*, 811-819.
Woodbury, R. G., Everitt, M. T., Sanada, Y., Katunuma, N., Lagunoff, D., & Neurath, H. (1978b) *Proc. Natl. Acad. Sci. U.S.A. 75*, 5311-5313.
Woodbury, R. G., Everitt, M. T., & Neurath, H. (1981) *Methods Enzymol. 80*, 588-609.
Yasutake, A., & Powers, J. C. (1981) *Biochemistry 20*, 3675-3679.
Yoshida, N., Everitt, M. T., Neurath, H., Woodbury, R. G., & Powers, J. C. (1980) *Biochemistry 19*, 5799-5804.
Yoshimura, T., Barker, L. N., & Powers, J. C. (1982) *J. Biol. Chem. 257*, 5077-5084.
Zimmerman, M., Morman, H., Mulvey, D., Jones, H., Frankshun, R., & Ashe, B. M. (1980) *J. Biol. Chem. 255*, 9848-9851.

Nuclear Magnetic Resonance and Neutron Diffraction Studies of the Complex of Ribonuclease A with Uridine Vanadate, a Transition-State Analogue

Babul Borah,[‡] Chi-wan Chen,[‡] William Egan,[§] Maria Miller,[∥] Alexander Wlodawer,[∥] and Jack S. Cohen*[,‡]

Biophysical Pharmacology Section, Clinical Pharmacology Branch, National Cancer Institute, Office of Biologics Research and Review, Food and Drug Administration, and Laboratory of Molecular Biology, National Institute of Arthritis, Diabetes, and Digestive and Kidney Diseases, National Institutes of Health, Bethesda, Maryland 20205, and Center for Chemical Physics, National Bureau of Standards, Gaithersburg, Maryland 20899

Received July 10, 1984; Revised Manuscript Received November 5, 1984

ABSTRACT: The complex of ribonuclease A (RNase A) with uridine vanadate (U-V), a transition-state analogue, has been studied with ^{51}V and proton NMR spectroscopy in solution and by neutron diffraction in the crystalline state. Upon the addition of aliquots of U-V at pH 6.6, the C^{ϵ}-H resonances of the two active-site histidine residues 119 and 12 decrease in intensity while four new resonances appear. Above pH 8 and below pH 5, these four resonances decrease in intensity as the complex dissociates. These four resonances are assigned to His-119 and His-12 in protonated and unprotonated forms in the RNase-U-V complex. These resonances do not titrate or change in relative area in the pH range 5-8, indicating a slow protonation process, and the extent of protonation remains constant with ca. 58% of His-12 and ca. 26% of His-119 being protonated. The results of diffraction studies show that both His-12 and His-119 occupy well-defined positions in the RNase-U-V complex and that both are protonated. However, while the classic interpretation of the mechanism of action of RNase based on the proposal of Findlay et al. [Findlay, D., Herries, D. G., Mathias, A. P., Rabin, B. R., & Ross, C. A. (1962) *Biochem. J. 85*, 152-153] requires both His-12 and His-119 to be in axial positions relative to the pentacoordinate transition state, in the diffraction structure His-12 is found to be in an equatorial position, while Lys-41 is close to an axial position. Hydrogen exchange data show that the mobility and accessibility of amides in the RNase-U-V complex do not significantly differ from what was observed in the native enzyme. The results of both proton NMR in solution and neutron diffraction in the crystal are compared and interpreted in terms of the mechanism of action of RNase.

The structure and mechanism of action of ribonuclease (RNase)[1] continue to be subjects of active interest. The recent reinvestigation of crystals of RNase A by X-ray diffraction (Wlodawer et al., 1982) and by neutron diffraction (Wlodawer & Sjolin, 1983) clarified certain features of the structure of the active site. In general, this provided a coherent picture of the structure as interpreted by both diffraction and proton NMR solution studies (Cohen & Wlodawer, 1982). A somewhat unusual finding of the NMR studies was the ab-

[‡] National Cancer Institute.
[§] Food and Drug Administration.
[∥] National Bureau of Standards.

[1] Abbreviations: RNase, ribonuclease; U-V, uridine vanadate; TSP, sodium 3-(trimethylsilyl)propionate-*2,2,3,3-d*$_4$; NOE, nuclear Overhauser enhancement; F, fermi unit of scattering length (10^{-13} cm).

sence of a significant effect on the ionization constants of the active-site histidine residues (12 and 119) upon complexation of RNase with a phosphonate analogue of the usual phosphate diester substrate (Griffin et al., 1973). This was in contrast to the large effects observed with several mononucleotides (Meadows et al., 1969, Ruterjans & Witzel, 1969; Wang & Haffner, 1973). It was, however, suggested that in the bipyramidal pentacoordinate transition state, direct interactions of the negatively charged oxygen atoms with catalytic side chains would occur (Griffin et al., 1973). The existence of an apparent transition-state analogue for RNase in the form of uridine vanadate (Lindquist et al., 1973; Alber et al., 1983; Wlodawer et al., 1983) has allowed us to test this hypothesis. This report focuses on the effect of uridine vanadate upon the His C^{ϵ} ring proton resonances.

The results are also compared with the detailed results of a neutron diffraction study of the RNase–U-V complex. We believe this is the first time that an enzyme transition-state analogue complex has been subjected to the combined analysis of both NMR solution studies and neutron diffraction studies of the crystal (Cohen & Wlodawer, 1982). The interpretation of the degree of protonation and the detailed juxtaposition of the two active-site histidine residues in the purported transition-state complex of RNase are found to require this combined approach. However, the results also provide a critical examination of transition-state analogues as a basis for assessing details of the enzyme mechanism.

Experimental Procedures

Bovine pancreatic ribonuclease A used in the NMR experiments was purchased from Boehringer Mannheim and was not further purified. The material was lyophilized 4 times from 99.75% D_2O (Bio-Rad). Samples for NMR studies were made by dissolving RNase in 0.5 mL of D_2O (100% Merck) with RNase concentrations in the 2–3 mM range and buffered with 0.2 M sodium acetate-d_3. pH measurements were made with a Model 26 pH meter (Radiometer). Direct meter readings in D_2O are reported. pH adjustments were made by adding 0.1–0.5 N NaOD and 0.25–1 N DCl.

Uridine vanadate was prepared by mixing solutions of uridine (Calbiochem) in D_2O and ammonium vanadate (Fisher Scientific Co.) in *hot* D_2O in the ratio of 1.4:1 of uridine to vanadate. Aliquots of a ca. 14.4 mM solution of uridine vanadate with a slight excess of uridine were then added to RNase A solutions.

^{51}V NMR experiments were carried out on a Bruker WM300 NMR spectrometer operating at a frequency of 78.91 MHz. Spectral conditions were the following: 10-kHz spectral window; 4K data points; 0.2-s acquisition time; 25-μs (60°) pulse; 0.4-s pulse repetition time. Prior to Fourier transformation, the free induction decay signal was zero filled and exponentially multiplied so as to result in a 5-Hz line broadening in the frequency domain signal.

Proton NMR spectra were recorded at 500 MHz on a Nicolet NT500 spectrometer interfaced to a Nicolet 1280 computer and a 293C pulse programmer. The strong signal from residual HDO was removed by using a gated decoupling technique. A total of 200–400 transients were accumulated with a spectral window of 6 kHz in 16K data points. The chemical shift values reported are downfield with respect to TSP at an ambient temperature of 24 ± 1 °C.

Curve fitting was carried out with the DEC PDP10 computer at the Computer Division, NIH, using the MLAB program.

The experimental procedures used in the neutron diffraction investigation have been fully described previously (Wlodawer et al., 1983) and therefore will not be repeated here.

Results

^{51}V NMR Results. The spectrum of a 5 mM solution of ammonium vanadate showed the presence of several components, the most intense of which is presumably $[H_2VO_4]^-$ (Heath & Howarth, 1981) and was assigned an arbitrary position of 0 ppm. The remaining resonances accounted for ca. 20% of the total signal intensity and were located at −8.5, 4.4, and 18.2 ppm (Figure 1). Upon addition of uridine, these signals decreased, and a uridine vanadate signal appeared downfield at ca. 54 ppm (Figure 1). This U-V signal was relatively broad, reflecting an increased rotational reorientation correlation time and an increased electric field gradient at the vanadate nucleus. At a stoichiometry of uridine to vanadate of approximately 1.2:1, the uridine vanadate complex was the predominant species in solution (>85% of the total). Upon addition of ribonuclease A to the solution, two things were observed to happen to the U-V resonance. First, the absolute intensity of the signal decreased in proportion to the amount of ribonuclease added; second, the line width at half-height of the remaining signal increased. These observations are readily accounted for; the loss of the U-V signal is explained by site-specific, tight binding of the U-V complex to ribonuclease (Lindquist et al., 1973). The effect of the greatly increased correlation time of the U-V complex when bound to the protein (τ_c ca. 10^{-8} s) would be to broaden the ^{51}V signal beyond detection on a high-resolution spectrometer, this loss of signal would be directly proportional to the amount of added enzyme. The broadening of the remaining U-V signal is due to nonspecific, weak binding of the complex to RNase. A direct proportionality between the amount of added enzyme and the line width of the remaining U-V complex is not expected, since the concentration of U-V is changing as enzyme is added.

Proton NMR Spectra of the RNase–U-V Complex. Figure 2 shows representative spectra of *free RNase* (3.02 mM) as well as spectra taken in the presence of increasing amounts of uridine vanadate at a pH of 6.64 ± 0.04. With additions of aliquots of uridine vanadate, the C^{ϵ} proton resonance of His-105 remained unaffected, whereas those of His-119 and His-12 decreased in intensity and disappeared when the concentration ratio of U-V to RNase exceeded unity. Four new resonances appeared at 7.61, 7.84, 8.57, and 8.85 ppm and grew slowly in intensity as the concentration of U-V was increased. It is apparent that the active-site histidine residues 119 and 12 are involved in complexing with the U-V inhibitor. With successive additions of the inhibitor, the areas of the *uncomplexed* His-119 and -12 C^{ϵ}–H resonances at 8.32 and 8.01 ppm, respectively, were monitored relative to that of the His-105 resonance at 8.43 ppm, which was unaffected by the complexation. The contributions from the broad NH peaks at ca. 8.32, 8.01, and 7.61 ppm were subtracted in determining the relative areas. As shown in Figure 3, the decreases in area of the *uncomplexed* His-119 and His-12 resonances were *not* equivalent to the rate of growth of any one of the *new* resonances of the RNase–U-V *complex*. Proton NMR experiments were also performed with the RNase–U-V complex in the presence of a large excess of uridine with a uridine to vanadate ratio of ca. 2:1. Similar results were obtained with four new resonances derived from the complex. These spectra are, however, unsuitable for quantitative analysis as the uridine aromatic ring proton resonance at ca. 7.9 ppm obscures the complex resonance at 7.84 ppm. Proton NMR spectra observed for RNase in the presence of a 2–3-fold excess of uridine alone show no effect on the histidine C^{ϵ}–H resonance, indi-

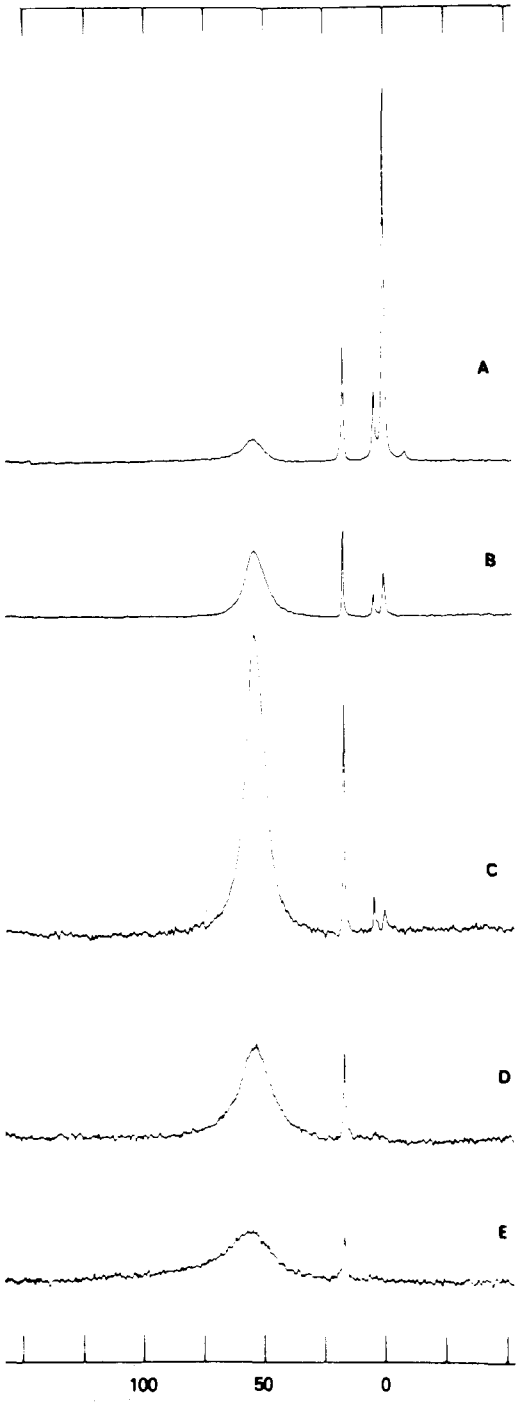

FIGURE 1: (A) ^{51}V NMR spectrum of a solution (5 mM) of a 1:1 mixture of ammonium vanadate and uridine in sodium acetate (0.2 M) buffer at pH 6.8; (B) as in (A) but with addition of uridine (1:1.4 vanadate:uridine); (C) as in (B) except that the ratio of vanadate to uridine was 1:2.6; (D) as in (C) but with the addition of RNase to 2.0 mM; (E) as in (D) but with additional RNase (3.5 mM). Details of spectral accumulation are in the text; spectra are shown in the absolute-value mode, and the vertical intensity has been multiplied times 4 in (C–E).

cating the absence of complexation between these species. Aliquots of ammonium vanadate when added to RNase also did not have any effect on the histidine ring proton resonances.

Assignments of Complex Resonances. Assignments of the resonances of the complex were made by selective deuterium exchange and by saturation transfer experiments. The histidine ring protons of RNase A were selectively deuterated at 37 °C at pH 8.9 for 11 days, as described previously (Shindo et al., 1976). The NMR spectrum of the selectively deuterated species adjusted to pH 6.6 shows that His-105 is completely

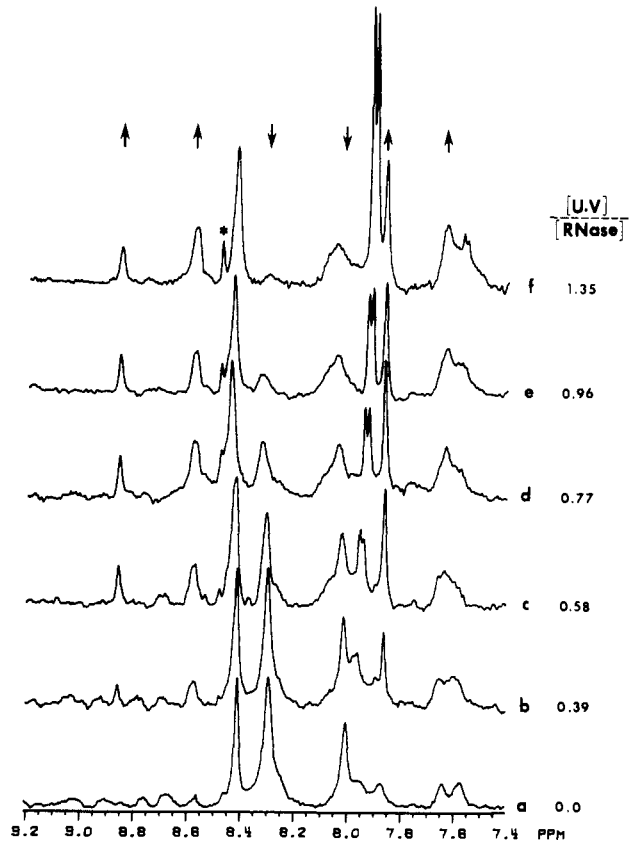

FIGURE 2: Proton NMR spectra at 500 MHz of RNase A in the presence of uridine vanadate (U-V). (a) Spectrum of free RNase, showing His ring proton resonances at 8.43 (His-105), 8.32 (His-119), and 8.01 (His-12) ppm at pH 6.64. (b–f) Spectra illustrating the effect of successive additions of U-V on His ring proton resonances. The ratio of [U-V] to [RNase] is shown at the right. The downward arrows indicate the disappearances of free His-119 and His-12 resonances, as [U-V] is increased. The upward arrows indicate the growth of four resonances due to the complex, as described in the text. The peak at 8.46 ppm designated by the asterisk is due to contamination. The doublet at 7.95 ppm originates from the uridine ring protons.

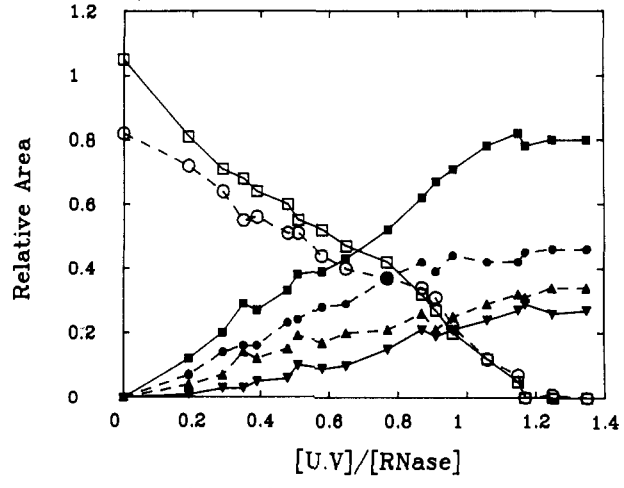

FIGURE 3: Integrated areas of His-119 and His-12 resonances in the RNase–U-V complex relative to the area of His-105, which is unaffected by addition of U-V. Relative areas of free His-119 (□) and free His-12 (○) resonances decrease with successive additions of U-V and are lost for [U-V]/[RNase] > 1.35. The relative areas for resonances of the complex at 7.61 (▲), 7.84 (■), 8.57 (●), and 8.85 (▼) ppm grow as U-V is added and become constant for [U-V]/RNase > 1.2.

deuterated and His-119 is largely deuterated but that His-12 remains protonated (Figure 4A) (note that His-48 is not observed at this pH). After addition of uridine vanadate (with

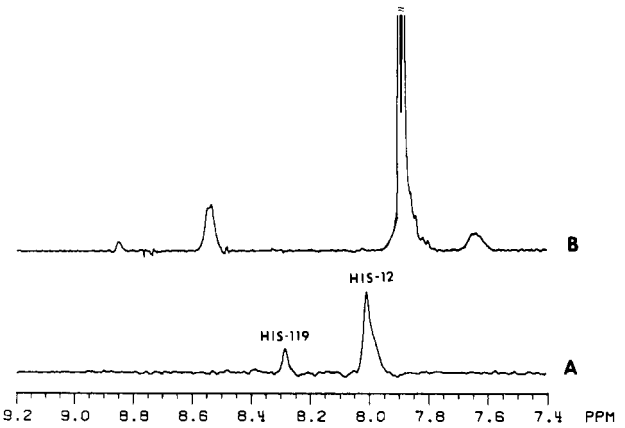

FIGURE 4: Proton NMR spectra at 500 MHz of deuterium-exchanged RNase A at pH 6.6 (A) and of RNase A complexed with U-V at pH 6.6 (B). The assignments of the resonances at 7.61, 8.57, and 8.85 ppm are described in the text; the strong resonance at 7.9 ppm arises from the uridine ring protons.

uridine:vanadate = 2:1), we observe two major resonances at 8.57 and 7.61 ppm, with relative areas similar to those shown in Figure 3. These two resonances can be firmly assigned to His-12 in the protonated and unprotonated states, respectively. The weak downfield peak at 8.85 ppm must originate from the residual His-119, as suggested by its at least 7–8-fold reduction in integrated area relative to the complexed His-12 resonance at 8.57 ppm. The fourth complex His resonance at 7.84 ppm is obscured by the strong uridine ring proton resonances.

From saturation transfer experiments, the assignment of the most intense of the complex resonances, at 7.84 ppm, can be decisively assigned to the deprotonated form of His-119 in the complex. In a mixture of uncomplexed and complexed RNase, the free His-119 resonance (at 8.32 ppm) was irradiated for 100 ms using the homonuclear decoupling channel, while observing the effect on the complex resonances. As seen in Figure 5, the 7.84 ppm resonance has clearly decreased in intensity, indicating slow chemical exchange with free His-119. A similar, but smaller, effect is visible for the 8.85 ppm resonance. Similar saturation transfer experiments for the His-12 resonance were unsuccessful, presumably due to differences in exchange rates.

The possibility that the four resonances of the complex arise from two different conformations of His-119 and His-12, respectively, can be ruled out from the effect of increasing temperature on the spectra. As the temperature is raised (Figure 6), chemical shift changes occur in all the His resonances, with the His-119 peak at 7.84 ppm shifting underneath the strong uridine peak. However, the four resonances of the complex are clearly discernible even at high temperature. Consequently, we can conclude that these two pairs of resonances represent the protonated and unprotonated forms of the two active-site histidine residues in slow exchange in the complex. These assignments also agree well with the relative area measurements shown in Figure 3. Within the experimental error of 5–10%, the areas under the curves assigned to His-119 in the complex account for all the original His-119 peak area. Similarly, adding the area under the curves assigned to His-12 in the complex can account for all the His-12 resonance.

Titration of Histidine C$^{\epsilon}$ Ring Protons. NMR titration data of the four histidine C$^{\epsilon}$ ring proton resonances of RNase A in sodium acetate solution (0.2 M) were obtained at an RNase concentration of 3.02 mM. The data were fitted with the theoretical model described previously, in which the resonances

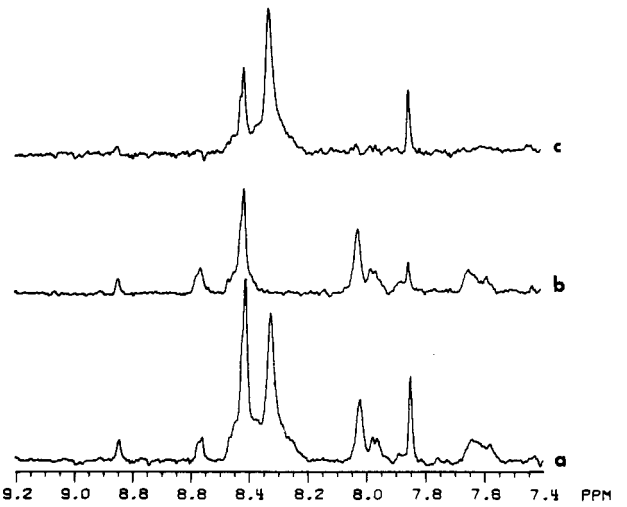

FIGURE 5: Saturation transfer proton NMR spectra of the RNase–U-V complex with [U-V]/[RNase] = 0.4. (a) Spectrum showing resonances of the complex as described in Figure 2, as well as uncomplexed His-105, His-119, and His-12 resonances at 8.43, 8.32, and 8.01 ppm, respectively. (b) Spectrum after irradiation for 100 ms at 8.32 ppm of the uncomplexed His-119 resonance. The resonance at 7.84 ppm has decreased considerably in intensity, while a smaller effect is observed for the 8.85 ppm resonance. (c) Difference spectrum of (a) and (b), illustrating the exchange NOE effect on the RNase–U-V complex resonances at 7.84 and 8.85 ppm. The residual intensity for the His-105 resonance at 8.43 ppm arises due to the proximity with the His-119 resonance being irradiated.

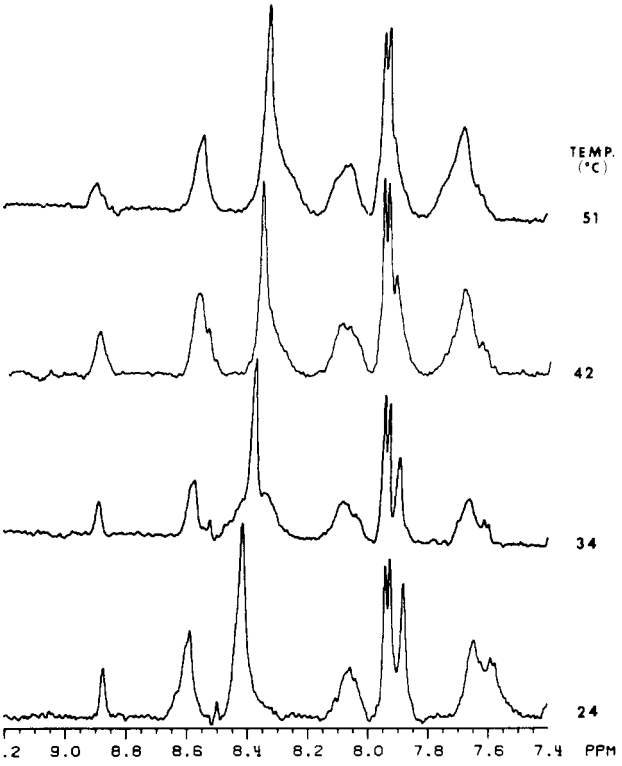

FIGURE 6: Proton NMR spectra of the RNase–U-V complex at different temperatures.

of His-12, -119, and -48 are fitted with the sum of two separate ionizations, while that of His-105 requires only a single ionization transition (Shindo & Cohen, 1975). Table I lists the pK_a values obtained from the present and previous work. It is noted that there is a small but significant concentration effect on the pK_a values, mostly for His-119.

Figures 7 and 8 show the pH titration data for histidine C$^{\epsilon}$ proton resonances in a solution that is 3.02 mM in RNase and 4.08 mM in U-V (i.e., [U-V]/[RNase] = 1.35). At pH ca.

Table I: Ionization Constants of Histidine Residues from Curve Fitting[a]

[RNase] (mM)	His-105	His-119		His-12		His-48	
	pK_1	pK_1	pK_2	pK_1	pK_2	pK_1	pK_2
2.2	6.90 ± 0.02	3.97 ± 1.62	6.58 ± 0.03	4.24 ± 0.38	6.23 ± 0.03	4.61 ± 0.24	6.53 ± 0.04
3.02	6.97 ± 0.02	4.29 ± 0.80	6.75 ± 0.02	3.36 ± 0.21	6.31 ± 0.02	4.90 ± 0.23	6.36 ± 0.06
previous values[a]	6.82 ± 0.02	4.12 ± 0.30	6.35 ± 0.21	4.11 ± 0.16	6.06 ± 0.09	4.74 ± 0.22	6.31 ± 0.08
RNase + U-V	6.92 ± 0.02						

[a] See Cohen & Shindo (1975).

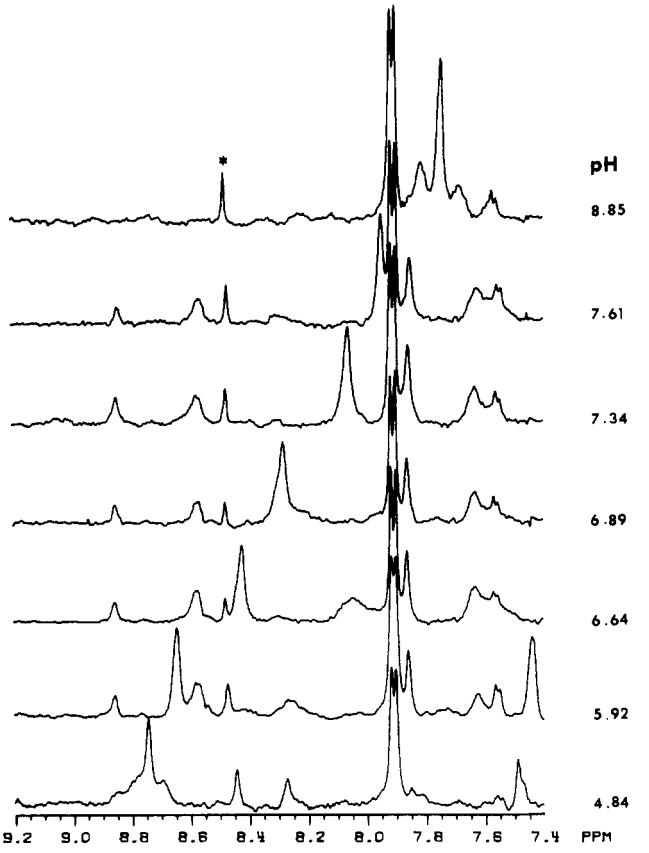

FIGURE 7: pH dependence of the proton NMR spectra of the RNase–U-V complex (details in text). The peak at 8.46 ppm designated by the asterisk is due to contamination.

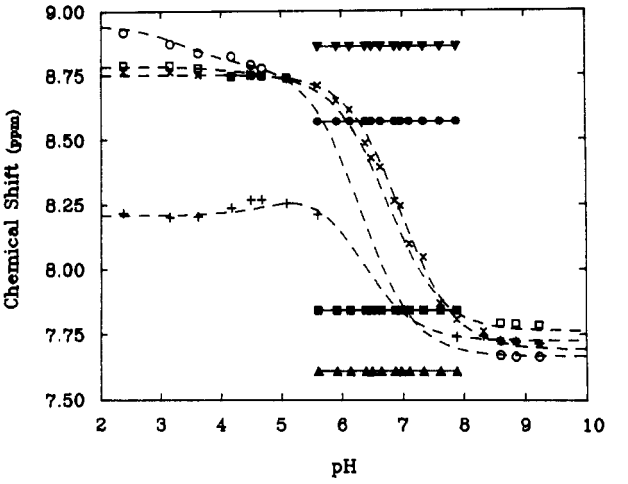

FIGURE 8: Proton NMR titration data of the RNase–U-V complex. The four resonances of the complex at 7.61, 7.84, 8.57, and 8.85 ppm remain unshifted in the pH range 5.1–8. The titration curves (---) for the His C^{ϵ} protons in free RNase A are shown for comparison: His-12 (○); His-119 (□), His-105 (×); His-48 (+); His-12 in complex (●, ▲); His-119 in complex (■, ▼).

6.6, Figure 7 shows the uncomplexed His-105 at 8.43 ppm and the four complex resonances as assigned above. As the pH is changed, His-105 (and His-48 where it is detectable) titrates in the usual way with pK_1 (His-105) ca. 6.92 ± 0.02, comparable to the pK_1 value in *free* RNase. The new His-119 resonances at 7.84 and 8.85 ppm and the His-12 resonances at 8.57 and 7.61 ppm, however, do not titrate in the pH range of ca. 5.1–8.0. Thus, the normal protonation–deprotonation process of the imidazole ring of the histidine residues at positions 119 and 12 is inhibited by complex formation. From the constant relative peak areas in this pH range, we can conclude that His-12 is 58% protonated and His-119 is 26% protonated. Another significant observation is that the complex between RNase and uridine vanadate is stable only in the pH range of ca. 5.1–8.0. Above and below this pH range, the complex dissociates as judged by the disappearance of the resonances at 8.85, 8.57, 7.84, and 7.61 ppm. As seen in Figures 7 and 8, at pH values below ca. 5.1 and above ca. 8.0, the His-119 and His-12 resonances titrate as in free RNase. The proton NMR spectrum indicates no degradation of RNase, and upon reversal of the pH back to the pH 5–8 range the complex peaks are again observed.

Proton Resonances Other than Histidine. Lenstra et al. (1979) have assigned the Phe-8, Phe-120, and Phe-46 proton resonances of RNase. They also reported that on addition of active-site inhibitors (e.g., 2′-CMP and 2′-UMP), all phenylalanine resonances broadened or disappeared. The resonance observed to be most affected (6.83 ppm) was assigned to Phe-20, and a new resonance at ca. 6.3–6.5 ppm was assigned to Phe-120 of the RNase–inhibitor complex. Both resonances of Phe-8 and Phe-120 were profoundly affected by U-V complexation, and Phe-46 was affected to a lesser extent. There are new resonances at 6.06 and 5.51 ppm. The Lys $C^{\epsilon}H_2$ composite resonance in the aliphatic region (ca. 3 ppm) of RNase spectra did not show any significant characteristic change or shift upon formation of the uridine vanadate complex.

Neutron and X-ray Refinement. The structure of the complex of ribonuclease A with uridine vanadate, based on the results of joint neutron and X-ray refinement with the diffraction data extending to 2.0-Å resolution, has been described before (Wlodawer et al., 1983). That communication was based on the results of preliminary refinement which has since been continued and has now been completed. All the diffraction data and procedures used in the current work are the same as those used previously. There were several aims of the further refinement: (1) to correct any remaining errors in the structure of the protein; (2) to check the unexpected features of the geometry of the active site and to confirm the details of the interactions between the enzyme and the transition-state analogue; (3) to ascertain the protonation state of histidine-12 and-119; (4) to reinvestigate the structure of the bound solvent; (5) to compare the pattern of amide hydrogen exchange with that of the native enzyme.

Only very few changes to the structure of the enzyme itself resulted from the current refinement. The most important of these was a reinterpretation of a loop region containing the

groups Gly-88 and Ser-89. The torsion angles σ and ψ, respectively, for these two amino acids were –69°, 161° and 92°, –32° both in the final model of the native enzyme (Wlodawer & Sjolin, 1983) and in the complex (Wlodawer et al., 1983). The electron density and nuclear density agreed reasonably well with that interpretation. Some doubt remained, however, since several tetrahedral angles were strained and the presence of a hydrogen rather than deuterium was indicated for the main-chain amide of Ser-89. Experimentally, we turned the peptide of Gly-88 and found that the resulting structure still fit the density well, while the strained angles were removed by further refinement. The amide of Ser-89 now appeared to contain a deuterium atom in agreement with the lack of protection from exchange expected for that part of the structure (see below). The new torsion angles (–67°, –14° and –90°, –4°) are also in good agreement with the independently refined model of Borkakoti et al. (1984). This modification did not result, however, in any decrease of either X-ray or neutron R factors, which were 0.188 for the X-ray data and 0.199 for the neutron data, respectively.

Protonation of Active-Stite Histidines Observed in Neutron Maps. In previous work concerning the structure of this complex, we expected to find one of the histidines-12 and -119 positively charged, while the other would be singly protonated (Lindquist et al., 1973). This was, however, not the case, and we found both histidines to be fully protonated. One of the aims of the current refinement was to reinvestigate these two histidines in order to rule out any errors caused by wrong interpretation, biased refinement, or other causes. Kossiakoff & Spencer (1981) have shown that the protonation state of a histidine can be established with high confidence on the basis of a neutron map phased without the hydrogens in question and by putting alternative structures into the refinement and examining the results. This approach taken by us was to remove both labile protons from each histidine, run several cycles of refinement, and examine the resulting difference Fourier maps or, alternatively, to fix the positional and the thermal parameters of all atoms in the structure and to refine the occupancy of all atoms. The latter procedure was successful in establishing the exchange state of amide hydrogens. The results of both procedures showed the clear presence of two deuterium atoms bound to the nitrogens of the imidazole groups of His-12 and His-119. The maps shown in Figure 9 were calculated with the phases which excluded the contributions of His-12, His-119, and uridine vanadate. The positive density indicates the presence of two deuteriums in each imidazole. Thus, our previous assertion about the protonation states of these groups important for catalysis still stands. The results of the NMR study appear to be partially consistent, as will be discussed below.

Geometry of the Active Site. It was more difficult to establish the details of the geometry of uridine vanadate and the nature of its interactions with amino acids of the enzyme. The structure of uridine vanadate itself has never been determined crystallographically. Furthermore, we were unable to find any reports of structures of vanadium-containing nucleotides. Only a few reports are available describing the structures of compounds containing pentacoordinated vanadium (V) in the form of a trigonal bipyramid, and none were similar enough to the case under study to provide a model necessary in the restrained refinement. For these reasons, we had to rely only on the X-ray and neutron maps (not necessarily completely unambiguous at 2-Å resolution) and on theoretical considerations (Lindquist et al., 1973). While the position and orientation of some part of the nucleotide, such as the uridine base, were

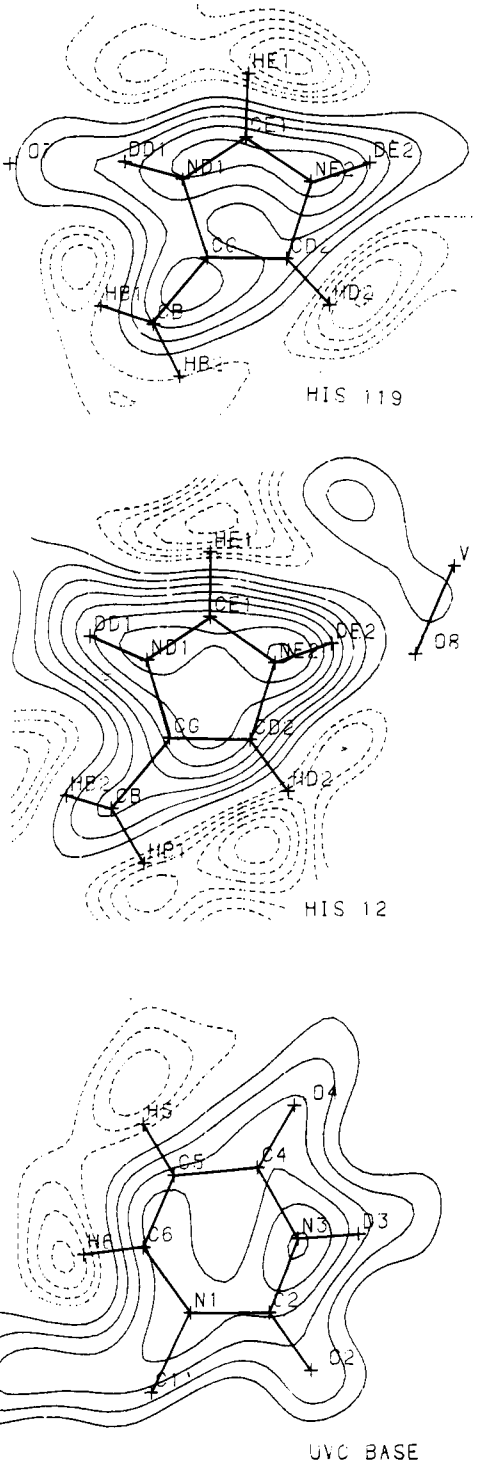

FIGURE 9: Neutron $F_o - F_c$ difference Fourier maps of His-12, His-119, and uridine base. All maps were calculated by using the final refined model for the RNase–U-V complex, but the contributions of histidine side chains and of U-V were excluded from phase calculations: positive density contour every 0.5 F (solid lines): negative density contour every 0.25 F (dashed lines).

completely clear and unambiguous from the beginning (Figure 9), the structure of the sugar ring was less obvious, and we encountered some difficulties in interpreting the neighborhood of the vanadium atom. We built test structures of 3′-*endo*- and 2′-*endo*-uridine from the standard groups distributed with the program COREL S (Sussman et al., 1977) and found that only the former would fit both the X-ray and neutron densities. Nevertheless, the sugar ring was always slightly distorted after refinement and even at its completion deviates from the ideal geometry.

The position of the vanadium atom was very clear in the X-ray map, but since the neutron scattering length of vanadium is very close to zero, no information about this atom can be found in the neutron map. Densities corresponding to the surrounding oxygens were also much clearer in the X-ray than in the neutron map. All the protein groups adjacent to the vanadate were very clear in both maps. The appearance of the active-site histidines was discussed above. Other side chains making direct contacts with the vanadate are Glu-11 and Lys-41. The position of the nitrogen NZ of Lys-41 was very clear, particularly in the neutron map, due to its high scattering length and the presence of three bound deuteriums. One of the deuteriums was observed to form a very clear hydrogen bond to the oxygen O2′ of the nucleotide. In the final refinement, the distance between NZ of Lys-41 and O2′ of uridine vanadate was 2.76 Å, practically unchanged from the value reported previously. The angle NZ–DZ2–O2′ was 174°, indicating a strong hydrogen bond. The presence of a hydrogen bond between these atoms was also confirmed by the appearance of the neutron map, in which they were connected by a continuous density, characteristic at this resolution. While the interaction of Lys-41 with the apical oxygen of the bipyramid is very clear, there is no sign of direct interaction with any equatorial oxygens. The distance between NZ of Lys-41 and the nearest of them, O6, is 3.4 Å. Of course, since both the vanadate and the lysine are charged, an ionic interaction is present, but the principal interaction appears to be with the apical ligand rather than with the equatorial one.

The ϵ-amino group of Lys-41 makes another strong hydrogen bond to the side chain of Asp-44. The distance between NZ 41 and OD1 44 is 2.77 Å, and the angle NZ–DZ1–OD1 is 161°. It should be stressed that equivalent hydrogen bonds are also present in the native structure, in which a phosphate ion is found in the active site. The distances between the hydrogen-bonded atoms are slightly longer in the latter case (3.02 and 2.94 Å for the bonds to the phosphate oxygen and to OD1 44, respectively), but that difference by itself could not explain the large difference of temperature factors of Lys-41 (see Discussion).

The arrangement of the imidazole nitrogens in histidines-12 and -119 also departs from the simple model in which they were expected to form the best possible contacts with the two apical oxygens of the vanadium bipyramid in order to facilitate proton transfer. While the nitrogen ND1 of His-119 forms a good hydrogen bond with the apical oxygen O7 (distance 2.96 Å, ND1–DD1–O7 angle 163°) it is still closer to the equatorial oxygen O3′ (distance 2.65 Å, but the ND1–DD1–O3′ angle of 119° is much less indicative of a hydrogen bond). The nuclear density also strongly favors the former interaction over the latter. The situation is even more confusing in the case of His-12. As reported previously (Wlodawer et al., 1983), the most obvious interaction is a clearly visible hydrogen bond between NE2 and the equatorial oxygen O8. The bond length is 2.69 Å, and the NE2–DE2–O6 angle is 134°. The nuclear density is clearly visible along this bond. Nevertheless, the apical oxygen O2′ is only 3.0 Å from NE2, and the angle NE2–DE2–O2′ is 122°. While no density corresponding to that bond is visible, the distance between NE2 12 and O2′ of the sugar is close enough to allow easy proton transfer.

One more side chain making a clear hydrogen bond with the vanadate oxygen is Gln-11, which is found in the vicinity of the equatorial oxygen O6. The distance between NE2 11 and O6 is 2.53 Å, and the angle NE2–DE22–O6 is 140°. The role of this side chain in the catalytic mechanism of RNase (if any) has not been considered previously. Finally, the

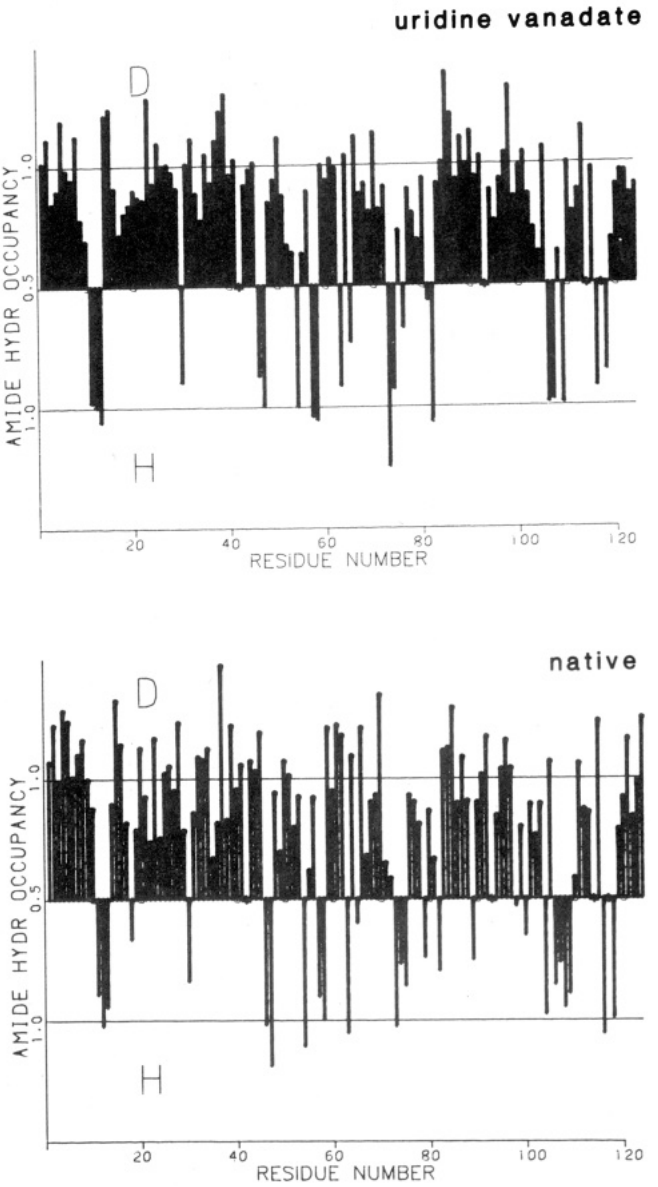

FIGURE 10: Comparison of the protection of the amide hydrogen from exchange in the native RNase and in the U-V complex. Bars above the horizontal lines show the calculated occupancy of amide deuterons (exchanged) while the occupancy of the protonated hydrogens can be read below the lines. Bottom panel, native RNase from Wlodawer & Sjolin (1983); top panel, RNase–U-V complex (this work).

main-chain amide nitrogen of Phe-120 is within a hydrogen bond distance (2.88 Å) of the equatorial oxygen O8, and the angle N120–D120–O8 is 162°. Again, no role has been postulated for this interaction.

Amide Hydrogen Exchange. A comparison of the pattern of hydrogen exchange between the native RNase and between the uridine vanadate–protein complex can yield information on whether the dynamic state of the protein is affected by inhibitor binding. A neutron diffraction study of hydrogen exchange in the native enzyme was reported by Wlodawer & Sjolin (1982, 1983). Occupanices of amide hydrogens (or deuteriums) were obtained in a refinement in which all positional and thermal parameters for the model were kept constant and only the occupancies of all atoms were allowed to vary. The estimated occupancy errors were ±15%. Nineteen amides were found to be fully protected in the native RNase (more than 80% H), and eight were partially exchanged (40–80% H). The results obtained in this study for the RNase–uridine vanadate complex are quite similar (Figure

10). We found 17 fully protected amide hydrogens and 3 which were partially protected from exchange. Fully protected peptides include residues 11, 12, 13, 30, 46, 47, 54, 57, 58, 63, 73, 74, 82, 106, 107, 109, 116, and 118, while residues 65, 76, and 81 were found to be partially protected. Three amides (75, 104, and 108) reported as fully protected in native RNase are not protected in the complex, while five amides found to be partially protected in the native enzyme (18, 79, 89, 98, and 100) are also not protected. Amides 74 and 104 were reported as partially protected in the native enzyme and appear to be fully protected now, while amides 76 and 81 were previously fully exchanged and are now partially protected. We interpret these results as indicative of remarkably small (if any) differences between the dynamic properties of the native and complexed RNase. The apparent differences are magnified by the arbitrary classification of the amides into three classes and could be made even smaller if the cutoff points were slightly shifted. We have noted previously that the apparent protection of two amides (18 and 89) in the native enzyme must have reflected experimental errors, since both of them were fully exposed to solvent. These amides now appear to be fully exchanged, with the improvement for Ser-89 probably caused by the reinterpretation of the main chain in its vicinity, as was discussed above. Of all the amides reported as protected in the complex, only Tyr-76 is not involved in an obvious hydrogen bond. The pattern of exchange is identical in the helical region of the protein and quite similar in the β sheet, with the only overall difference seen in even less protection found in one half of the V forming the sheet than in the other half. Considering that the time spent on hydrogen exchange was less than that spent previously, while the individual exchange rates were increased by the increase in pH of the solution, we cannot consider these changes to be meaningful.

Discussion

The catalytic mechanism whereby RNase hydrolyzes ribonucleotide phosphodiesters is generally divided into two steps (Richards & Wyckoff, 1971). The first step is a transesterification of the 3′,5′-phosphodiester to a cyclic 2′,3′-phosphate. This step is facilitated by abstraction of a proton from the 2′-OH and donation of a proton to the 5′ leaving group. The second step of the catalytic reaction involves hydrolysis of the cyclic phosphate to yield a 3′-phosphate. This is catalyzed by donation of a proton to the 2′-ester group and abstraction of a proton from water. In each step, a general base abstracts a proton and a general acid donates a proton. These groups were shown to be in an on-line arrangement by the use of diastereoisomeric phosphorothioates (Usher et al., 1970a,b, 1972). Stated in another way, the proton-abstracting and the proton-donating groups are physically distinct in each of the forward and reverse reactions. Since each step must proceed via a pentacoordinate trigonal bipyramidal phosphorus transition state (or intermediate), this finding virtually eliminates the need to invoke pseudorotation of such intermediates in the mechanism (Westheimer, 1968; Usher et al., 1970a,b).

It has generally been considered that the two acid–base groups are histidines-12 and -119. RNase derivatives in which these two groups were chemically modified were found to be enzymatically inactive (Stark et al., 1961; Crestfield et al., 1963), although this is a somewhat ambiguous distinction (Bello & Nowoswiat, 1965). Several X-ray diffraction studies of RNases A and S implicated these His residues in the active-site region (Wykoff et al., 1970; Wlodawer, 1984). Recent crystallographic investigations of the structure of RNase resulted in a relatively unambiguous placing of these two groups within the active site (Wlodawer et al., 1982; Wlodawer & Sjolin, 1983). Their physical separation by the phosphate makes it extremely unlikely that these two groups could participate jointly in a catalytic mechanism (Witzel, 1963). There is also evidence from proton NMR studies of the C^{ϵ}–H resonances of these groups that there is no interaction between the two active-site His residues (Cohen & Shindo, 1975; Brauer & Benz, 1978).

It should be noted that several X-ray diffraction studies of RNase inhibitor complexes failed to provide an unambiguous understanding of the detailed mechanism of action [for a review, see Wlodawer (1984)]. In conjunction with a study by diffraction methods of the RNase–UV complex (Wlodawer et al., 1983), we undertook to investigate the effect of this transition-state analogue on the active-site His C^{ϵ}–H resonances in solution. The use of this analogue of the pentacoordinate transition state can be contrasted with other inhibitors studied by NMR [for a review, see Cohen et al. (1983)]. For example, mononucleotides show large effects of the negative charge upon the NMR titration curves of the active-site His resonances. However, these effects depend significantly on the pyrimidine or purine present and the position of phosphorylation on the ribose ring (Griffin et al., 1973). As such, the mononucleotides are poor models of the phosphate diester substrates. A dinucleoside phosphonate analogue, UpcA, which is not cleaved, showed no significant effect on the C^{ϵ}–H NMR titration curves (Griffin et al., 1973) or on the ^{13}C NMR titration curves of [ϵ-^{13}C]His-12 RNase S′ (Cohen et al., 1980). It was postulated that these histidine residues contact the phosphorus oxygens only in the transition state (Griffin et al., 1973). In other words, they play no significant role in the binding of the substrate but are involved only in catalysis. Under the conditions of our experiment, we found no effect of the substrate analogue 2′-FUpA (Antonov et al., 1978) on the active-site histidine resonances, although we had no evidence that this substance was binding.

The results presented here show significant shifts of the proton resonances of His-12 and -119 in the RNase–U-V complex. The resonances were assigned by deuterium-exchange and saturation-transfer experiments. The chemical shifts of the pair of resonances assigned to each of the two His residues in the pH range 5.1–8 are extremely similar to their respective chemical shifts in the uncomplexed fully protonated and unprotonated states (Figure 7). We therefore conclude that the four resonances observed represent very slowly exchanging (or nonexchanging) His-12 and His-119 in partially protonated/unprotonated forms in the RNase–U-V complex. The proportions of the protonated species are given in each case by the relative area of the downfield peak assigned to the protonated form of each of the active-site His residues. Since the degree of protonation for each of these imidazoles is different, this implies that four species of RNase–U-V complex may be present in solution at any one time, namely, species containing both protonated His-12 and protonated His-119, species with either one or the other His protonated, or species with His unprotonated. We cannot calculate the proportions of each of these species on the basis of the available data.

The diffraction studies attempted to answer several closely related questions concerning the mechanism of action of RNase. The stereochemistry of the active site of the enzyme in the presence of the transition-state analogue is shown diagrammatically in Figure 11. This reinvestigation of the structure of the complex confirmed our earlier assertion (Wlodawer et al., 1983) that it is Lys-41 rather than His-12 which makes a clear hydrogen bond to the apical oxygen of the trigonal bipyramid surrounding the vanadium atom, while

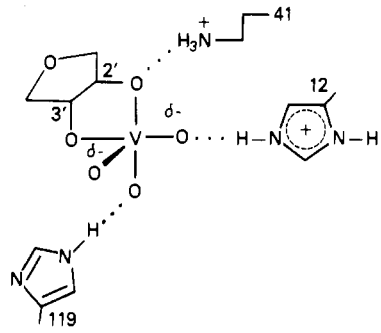

FIGURE 11: Diagrammatic representation of the RNase–U-V complex on the basis of the neutron diffraction and NMR studies. The predominant protonation states of the two active-site histidine residues as shown were determined from the NMR results. The neutron diffraction results indicated a greater degree of protonation of His-119 and showed the Lys-41 residue to be apical while the His-12 residue is equatorial.

His-12 is hydrogen bonded to the equatorial oxygen. On the surface, this observation should be taken as a contradiction of the accepted mechanism of action of the enzyme in which both histidine-12 and histidine-119 are involved in proton transfer, while the role of Lys-41 is to provide a rather unspecified stabilization of the transition-state complex (Alber et al., 1983). This is unlikely, however, since lysine cannot directly act as a general acid *and* a general base at the neutral pH in which our data were taken (and in which RNase is active). Rather, we should consider whether the design of the transition-state complex is such that the groups are *not* in the position of optimum binding and that our expectations to the contrary are unfounded. We should keep in mind that while there is no indication that His-12 forms a hydrogen bond with the apical oxygen of the bipyramid, the distance between NE2 and O2′ is only 3.0 Å, so proton transfer is quite possible.

It is still not clear what role is played by Lys-41 and how its close association with the reacting group can facilitate the proton shuttle. Incidentally, we have no simple explanation of the reasons for vastly diminished mobility of this side chain, as manifested by the drop of its temperature factor from over 20 $Å^2$ (for NZ) in the native enzyme to about 8 $Å^2$ in the complex. All other structures of the complexes of RNase with inhibitors show no such ordering of this residue. We might accept that the immobilization is somewhat caused by the rearrangement due to the presence of the transition-state analogue (Alber et al., 1983) but the types and lengths of the hydrogen bonds between NZ of Lys-41 and its neighbors are not very different in the complex and in the native enzyme, as was mentioned above. Another possibility is that this is an artifact introduced by the presence of vanadium rather than phosphorus and that this effect would not be observed in the true transition state. We know from comparison of the patterns of hydrogen exchange that the presence of the transition-state analogue does not affect long-range flexibility of the protein molecule, and this observation is in agreement with the results of chemical studies in the presence of other substrate analogues (Rosa & Richards, 1982). This does not rule out other, more localized changes, but Lys-41 was the only group for which a major change in mobility was detected.

The observed protonation states of both histidines need also to be clarified. Neutron maps showed that both histidines are doubly protonated, while only partial protonation was observed in the NMR experiments. It is clear that we are attempting to study a dynamic event and that the presence of the true transition-state analogue does not freeze the protonation of the histidines. While for the proton transfer to take place it is necessary that only one histidine be protonated for the forward reaction (and the other one for the reverse reaction), we observe experimentally the presence of species corresponding to both cases. We suspect that the NMR experiments give a more accurate picture of the events and that the true levels of protonation may be lower than those indicated by the neutron experiment. The fact that the NMR experiments were carried out in solution while the diffraction experiments were carried out in the solid state may be responsible for these differences. The finding that both active-site histidine residues are partially protonated in solution is consistent with their acid–base catalytic roles. while the U-V inhibitor is different from the true transition state, the proportions of the protonated species observed may be considered to be comparable to the instantaneous distribution of protons during the reaction catalyzed by the enzyme.

Registry No. RNase A, 9001-99-4; V, 7440-62-2; histidine, 71-00-1.

REFERENCES

Alber, T., Gilbert, W. A., Ponzi, D. R., & Petsko, G. A. (1983) *Ciba Found. Symp. 93*, 4–24.

Antonov, I. V., Gurevich, A. Z., Dudkin, S. M., Karpeisky, M. Y., Sakharovsky, V. G., & Yakovlev, G. I. (1978) *Eur. J. Biochem. 87*, 45–54.

Bellow, J., & Nowoswiat, E. F. (1965) *Biochim. Biophys. Acta 105*, 325–332.

Borkakoti, N., Moss, D. A., Stanford, M. J., & Palmer, R. A. (1984) *J. Crystallogr. Spectrosc. Res. 14*, 467–694.

Brauer, M., & Benz, F. W. (1978) *Biochim. Biophys. Acta 533*, 186–194.

Cohen, J. S., & Shindo, H. (1975) *J. Biol. Chem. 250*, 8874–8881.

Cohen, J. S., & Wlodawer, A. (1982) *Trends Biochem. Sci. (Pers. Ed.) 7*, 389–391.

Cohen, J. S., Niu, C.-H., Matsuura, S., & Shindo, H. (1980) in *Frontiers in Protein Chemistry* (Liu, T.-Y., Mamiya, G., & Yasunobu, K. T., Eds.) pp 3–16, Elsevier, New York.

Cohen, J. S., Hughes, L., & Wooten, J. (1983) in *Magnetic Resonance in Biology* (Cohen, J. S., Ed.) Vol. 2, pp 130–247, Wiley, New York.

Crestfield, A. M., Stein, W. H., & Moore, S. (1963) *J. Biol. Chem. 238*, 2421–2428.

Findlay, D., Herries, D. G., Mathias, A. P., Rabin, B. R., & Ross, C. A. (1962) *Biochem. J. 85*, 152–153.

Griffin, J. H., Schechter, A. N., & Cohen, J. S. (1973) *Ann. N.Y. Acad. Sci. 222*, 693–708.

Heath, E., & Howarth, O. W. (1981) *J. Chem. Soc., Dalton Trans.*, 1105–1110.

Kossiakoff, A. A., & Spencer, S. A. (1981) *Biochemistry 20*, 6462–6474.

Lenstra, J. A., Bolscher, B. G. J. M., Stob, S., Beintema, J. J., & Kaptein, R. (1979) *Eur. J. Biochem. 98*, 385–397.

Lindquist, R. N., Lynn, J. L., & Lienhard, G. E. (1973) *J. Am. Chem. Soc. 95*, 8762–8768.

Richards, F. M., & Wyckoff, H. W. (1971) *Enzymes, 3rd Ed. 4*, 647–806.

Rosa, J. J., & Richards, F. M. (1982) *J. Mol. Biol. 160*, 517–530.

Ruterjans, H., & Witzel, H. (1969) *Eur. J. Biochem. 9*, 118–127.

Shindo, H., Hayes, M. B., & Cohen, J. S. (1976) *J. Biol. Chem. 251*, 2644–2647.

Stark, G. R., Stein, W. H., & Moore, S. (1961) *J. Biol. Chem. 236*, 436–442.

Sussman, J. L., Holbrook, S. R., Church, G. M., & Kim, S. (1977) *Acta Crystallogr., Sect. A A33*, 800–804.

Usher, D. A., Richardson, D. I., & Eckstein, F. (1970a) *Nature (London) 228*, 663–665.
Usher, D. A., Richardson, D. I., Jr., & Oakenfull, D. G. (1970b) *J. Am. Chem. Soc. 92*, 4699–4711.
Usher, D. A., Erenrich, E. S., & Eckstein, F. (1972) *Proc. Natl. Acad. Sci. U.S.A. 69*, 115–118.
Wang, J., & Haffner, P. (1973) *Biochemistry 12*, 1608–1618.
Westheimer, F. H. (1968) *Acc. Chem. Res. 1*, 70–78.
Witzel, H. (1963) *Prog. Nucleic Acids Res. Mol. Biol. 2*, 221–258.
Wlodawer, A. (1984) in *Biological Macromolecules and Assemblies* (Jurnak, F., & McPherson, A., Eds.) Vol. 2, pp 393–439, Wiley, New York.
Wlodawer, A., & Sjolin, L. (1982) *Proc. Natl. Acad. Sci. U.S.A. 79*, 1418–1422.
Wlodawer, A., & Sjolin, L. (1983) *Biochemistry 22*, 2720–2728.
Wlodawer, A., Bott, R., & Sjolin, L. (1982) *J. Biol. Chem. 257*, 1325–1332.
Wlodawer, A., Miller, M., & Sjolin, L. (1983) *Proc. Natl. Acad. Sci. U.S.A. 80*, 3628–3631.
Wyckoff, H. W., Tsernoglou, D., Hanson, A. W., Knox, J. R., Lee, B., & Richards, F. M. (1970) *J. Biol. Chem. 245*, 305–328.

Some Kinetic Characteristics of Immobilized Protomers and Native Dimers of Mitochondrial Malate Dehydrogenase: An Examination of the Enzyme Mechanism†

George DuVal, Harold E. Swaisgood,* and H. Robert Horton
Departments of Biochemistry and Food Science, North Carolina State University at Raleigh, Raleigh, North Carolina 27695-7624
Received July 13, 1984

ABSTRACT: Some kinetic characteristics of immobilized native mitochondrial malate dehydrogenase dimers and immobilized protomers, prepared by direct immobilization under conditions yielding complete dissociation without substantial unfolding, were compared to those of native soluble enzyme. Enzyme was covalently immobilized to derivatized porous glass by using a technique which permitted subsequent release of bound enzyme with 0.2 M hydroxylamine at room temperature and pH 7. Kinetic properties of enzyme released from both immobilized dimers and protomers were the same as those for native soluble enzyme, indicating that the immobilization reaction per se did not affect the structure. Both immobilized native dimers and the immobilized protomers exhibited activity with a pH dependence similar to that of native soluble enzyme. The effects of diffusional inhibition were demonstrated for both forms of the immobilized enzyme, especially for the NADH → NAD^+ reaction direction. Intrinsic Michaelis constants of both immobilized forms, obtained by extrapolation of apparent values, were similar to those of the soluble enzyme. Furthermore, the effects of inhibitors and effectors with the immobilized forms were the same as those with native soluble enzyme. For example, substrate inhibition was observed with oxalacetate, the inhibitor hydroxymalonate was competitive with ketomalonate and uncompetitive with L-malate, and inhibition was observed with citrate in the NADH → NAD^+ direction. Thus, immobilization did not appear to suppress the conformational equilibria of either protomers or dimers. More significantly, the kinetic characteristics of the immobilized protomer were indistinguishable from those of the dimer. Hence, a reciprocating mechanism involving subunit interactions cannot be invoked to explain the allosteric behavior of this dimeric enzyme. Rather, the results are consistent with an equilibrium between two conformers as proposed by Mullinax et al. [Mullinax, T. R., Mock, J. N., McEvily, A. J., & Harrison, J. H. (1982) *J. Biol. Chem. 257*, 13233–13239], one of which preferentially binds citrate and NAD^+ while the other binds NADH.

Catalysis of reactions by enzymes attached to a surface may deviate in kinetic behavior from that observed for enzymes in solution, due both to substrate, product, or effector molecules' partitioning between the bulk phase and the surface and to diffusional limitations (Engasser & Horvath, 1973, 1974a–c; Goldstein, 1976; Taylor & Swaisgood, 1981; Cho & Swaisgood, 1974). If the enzyme has been chemically attached by covalent linkage, the immobilization reaction itself can also affect activity (Ollis & Datta, 1976; Mosbach, 1980; Bickerstaff, 1980). However, failure to consider the above effects can limit the information derived and possibly result in misinterpretations. Therefore, in this study, the effects of diffusional factors and the chemistry of immobilization were examined in an investigation of immobilized protomers and dimers of malate dehydrogenase (MDH).[1]

Malate dehydrogenase (L-malate:NAD^+ oxidoreductase, EC 1.1.1.37) is obtained as a dimer of two identical 35000-dalton subunits. MDH subunits immobilized on Sepharose have been shown to be active (Jurgensen et al., 1981). The kinetic properties of immobilized protomers and dimers were further

† Paper No. 9372 of the Journal Series of the North Carolina Agricultural Research Service. The use of tradenames in this publication does not imply endorsement by the North Carolina Agricultural Research Service of the products. This investigation was supported in part by National Institutes of Health Research Grant GM 28978.
* Address correspondence to this author at the Department of Food Science, North Carolina State University at Raleigh.

[1] Abbreviations: MDH, malate dehydrogenase; DTT, dithiothreitol; EDTA, ethylenediaminetetraacetic acid; EDC, 1-ethyl-3-[3-(dimethylamino)propyl]carbodiimide; OAA, oxalacetate; Tris, tris(hydroxymethyl)aminomethane; DTNB, 5,5′-dithiobis(2-nitrobenzoic acid).

0006-2960/85/0424-2067$01.50/0